

This discussion paper is/has been under review for the journal Ocean Science (OS).  
Please refer to the corresponding final paper in OS if available.

# Numerical modeling of dynamics of Russian south waters within the framework of operational oceanography tasks

A. V. Grigoriev<sup>1</sup>, A. G. Zatsepin<sup>2</sup>, V. A. Kubryakov<sup>1</sup>, I. V. Charikov<sup>1</sup>, and L. D. Fedotova<sup>1</sup>

<sup>1</sup>N. N. Zubov's State Oceanographic Institute, Moscow, Russian Federation

<sup>2</sup>Shirshov's Institute of Oceanology, Moscow, Russian Federation

Received: 17 December 2010 – Accepted: 30 June 2011 – Published: 29 August 2011

Correspondence to: A. V. Grigoriev (ag-privat@mail.ru)

Published by Copernicus Publications on behalf of the European Geosciences Union.

1865

## Abstract

Modeling of the Black Sea and Caspian Sea waters dynamics was conducted within the framework of the European ECOOP project and Russian project JISWO on the basis of the Princeton Ocean Model (POM). Nowcasting and tree days forecasting of the Black  
5 Sea dynamics was carried out in a daily mode with horizontal resolution of  $\sim 1$  km along the Russian coast of the basin. The nowcasting of the Caspian Sea dynamics was carried out every ten days with horizontal resolution of  $\sim 5$  km on the basis of climatic information about water temperature and salinity and decade-averaged wind NCEP-NCAR. Examples of calculations are presented here and their comparison with space  
10 remote sensing and in situ (hydrological measurements) data is fulfilled, and the results of model validation are discussed.

## 1 Introduction

Numerical modeling of the Black and Caspian seas' dynamics was fulfilled in the State Oceanographic Institute of Russian Federation (SOI) within the framework of the Eu-  
15 ropean ECOOP project (European COastal-shelf sea OPerational observing and forecasting system, 2007–2010 years) and the national project JISWO (Joint Information System on World Ocean). In both cases, a well-known numerical Princeton Ocean Model (POM, /1,5,6/), adapted for the regional conditions, was used.

The purpose of the paper is a description of the automated system of nowcasting  
20 and forecasting of hydrophysical parameters built during ECOOP and the estimation of quality of modeled fields. First of all, the system output in the Russian part of the Black Sea is described. These results were obtained in close co-operation with other participants of the project, particularly with the Marine Hydrophysical Institute of National Academy of Sciences of Ukraine, Sevastopol (MHI). The comparison of observations  
25 and modeled fields is also presented below. The results of the modeling of the Caspian Sea are presented in this paper. This work represents the Russian Federation in a

1866



been performed. Contact measurements (CTD) obtained by R/V *Professor Shtokman* of “Shirshov’s” Institute of Oceanology (IO RAS) for the period of 9 March until 2 April 2009 were used. In Fig. 5, the regions of R/V *Survey* and modeling are shown.

5 It should be noted at the beginning that some characteristics of water in the region in March should be reflected in the measurement data and modeling/7/. The vertical structure is an upper quasi-homogeneous layer (UQHL, several tens meters), thermo-  
halo- pycnocline below to depths of 500 m and the underlying quasi-homogeneous layer. The main feature of the vertical structure of the waters of the Black Sea is the  
10 so-called cold intermediate layer (CIL) with the axis at depths of 50–100 m depending on the point of observation. Rim Current has extending along the continental slope, roughly along the isobath 1200 m, and produces a general cyclonic circulation in the sea. In the area of the continental slope, the eddies with spatial scales of ~100 km are also observed, and directly in the shelf-slope zone – anticyclonic eddies with horizontal dimensions are about 10 km (see Fig. 2). These dynamic characteristics are reflected  
15 in the distributions of isolines in the cross-sections. Note also that the salinity is a major contributor to the spatial distribution of the density of Black Sea water, determining its dynamics. Therefore, profiles, sections and maps are constructed from the values of salinity, the most informative in analyzing the features of water dynamics in the region.

Vertical profiles built both from CTD and modeled data reflect the typical vertical  
20 structure of waters in the region in March (Fig. 6, for hydrological Station 5), in particular, the presence of the upper quasi-homogeneous layer (UQHL) with a capacity of ~40 m, the cold intermediate layer (CIL) with the axis at a depth of 60 m, the main pycnocline to depths of 500 m and the underlying quasi-homogeneous layer. The vertical profiles of salinity and density are of the same type because the water density  
25 in Black Sea is mostly defined by salinity. Qualitatively, the model and the observed profiles are very similar. For the salinity difference in values of the order of ~0.1 ‰, for the temperature there is the same order in degrees °C at depth. A maximum difference in temperatures is observed on a surface – approximately 1.5 °C.

1869

Distribution of thermohaline characteristics at a cross-section perpendicular to the coast (see Fig. 5) is typical for the Black Sea, and shows a decline in the depth of isolines from coast to the center of the sea, caused by a general cyclonic circulation (Fig. 7). The section shown in Fig. 7a is built from asynchronous CTD-data made by  
5 R/V *Professor Shtokman* in the period 10/03/2009–13/03/2009. Figure 7b is built from model data corresponding to the points and times of ship observations. Comparing Fig. 7a and b, we can conclude that the salinity distribution in sections are similar and have similar quantitative values. As the differences can be noted, large vertical salinity gradients in halocline on the cross-section, which was built from CTD-data. But reducing the spatial discreteness of the model data in the cross-section is well defined  
10 deflection contour lines in the shelf-slope (right side of Fig. 7c) due to the presence of the anticyclonic vortex with the spatial size of ~10 km (see Fig. 8a). A similar distribution of isolines on the edge of the continental slope of Black Sea is fixed often from CTD data of many hydrological surveys with a small horizontal step (~1 km).

15 Synoptic variability in space and time is clearly expressed in the model calculations of water dynamics in the region. As an example, the model velocity fields corresponding to the beginning and end of the hydrological survey R/V *Professor Shtokman* is shown in Fig. 8. With regard to estimates of the degree of differences of model and measured values, then, due to high degree of asynchrony of the hydrological survey, comparison between measured and modeled data does not make any sense. Therefore, the estimations of quality of modeling are possible using remote sensing. Examples of comparisons of modeled data with satellite observations are shown in Figs. 8, 9. Thus, synoptic eddies, reflected in the salinity field (model) and the concentration of chlorophyll A (satellite image) show a high correspondence in the spatial size and horizontal location (Fig. 9). The RMS of the difference between the model and the measured (Sea Surface Temperature, SST) temperature in area of modeling for 2 July, 2009, was equal to RMS = 1.1 °C (Fig. 10).

1870

As seen in the figures presented, some shift of location of  $T$ ,  $S$  anomalies in modeled calculations concerning supervision takes place. For elimination of this effect, data assimilation in a local model can be used (now it can only be assimilated in a basin-scale model).

5 It is also interesting to analyze how the magnitude of the errors of forecasting (Fig. 11) is dependent on the time of forecasting. This is done using the information about temperature and salinity at the moments of contact measurements (for Station 5). For temperature, the minimum number of errors takes place in the case of 1–2 days forecasting (except the depths below CIL, where variability is considerably low than within UQHL). In the upper layers, the forecasting is closer to measurements than nowcasting (0 days in the Fig. 11). It is worth mentioning the considerable errors of modeled temperature in the upper layer. (As the research of colleagues from MHI showed, this failing can be decreased by the division of the heat flow on the surface of the sea into long-wave and short-wave parts.) For salinity, the maximum of errors is located in the range of depths about 100–200 m (main halo- pycnocline). In the upper layers, the presence of local maximum of errors when forecasting for 2 days is distinct. But in general, a forecasting for 1 day (and at some depths for 3 days) does not yield or excels nowcasting in quality.

The reasons for such results could be following:

- 20 – Nowcasting during the Project was carried out by the model for the time span of 1 day. Possibly, this time is not enough and it is necessary to increase it up to 2 days.
- In addition, dynamic features of interaction between the currents and bottom relief and adaptation with the wind stress likely show up during the forecast, which finds display in the variability of profiles of temperature and salinity.

1871

### 3 Caspian Sea

The formal parameters of the numerical model were the following: the grid for calculation which covered the total water area of the sea had the dimensions  $243 \times 193 \times 18$  points and lay in borders of  $36.6^{\circ}$ – $47.0^{\circ}$  northern latitude and  $47.0^{\circ}$ – $54.0^{\circ}$  east longitude. The grid step was equal to 4.9 km in latitude and 3.7 km in longitude. The levels were thickening exponentially from the middle layers to the surface and to the bottom of the sea for the best resolution of the surface and bottom border layers. Initial temperature and salinity fields were climatic /3/, and have been time interpolated for every decade of the months. The data of NCEP/NCAR reanalysis was used for a daily pressure field over the Caspian Sea (<http://www.cdc.noaa.gov/cdc/reanalysis/reanalysis.shtml>), which was interpolated by means of splines on the chosen spatial grid. The wind stress fields were calculated according to the data about atmospheric pressure. Along with temperature and salinity fields, the wind stress fields are used as input data and are sufficient for every decade nowcasting calculations of the current fields in the Caspian Sea.

As well as for the Black Sea, the process includes several stages which have been completely automated. The stages are:

1. information read-out of atmospheric pressure over the Caspian Sea;
2. the calculation of the average decade fields of atmospheric pressure;
- 20 3. the calculation of the average decade wind stress according to the data about atmospheric pressure;
4. the placement of the files of initial (temperature, salinity) and boundary (wind stress) conditions in folders corresponding to each decade of the month;
5. realization of model calculations;
- 25 6. visualization of the results;

1872





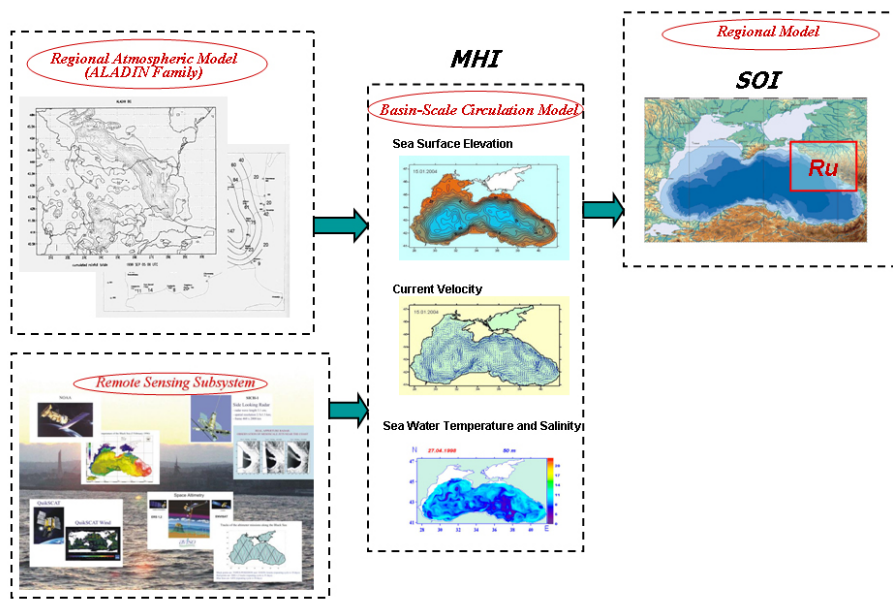


Fig. 1. System of nowcasting and forecasting of Black Sea water dynamics.

1877

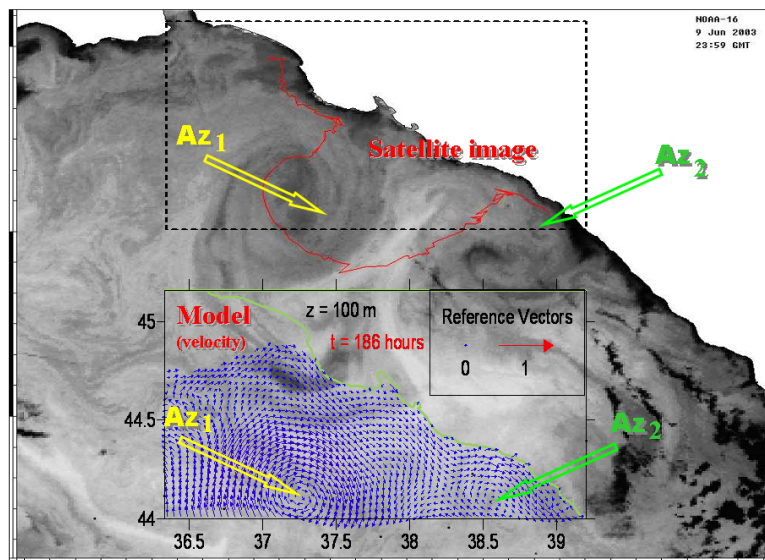


Fig. 2. Comparison of the modeled results (currents) with satellite image.

1878

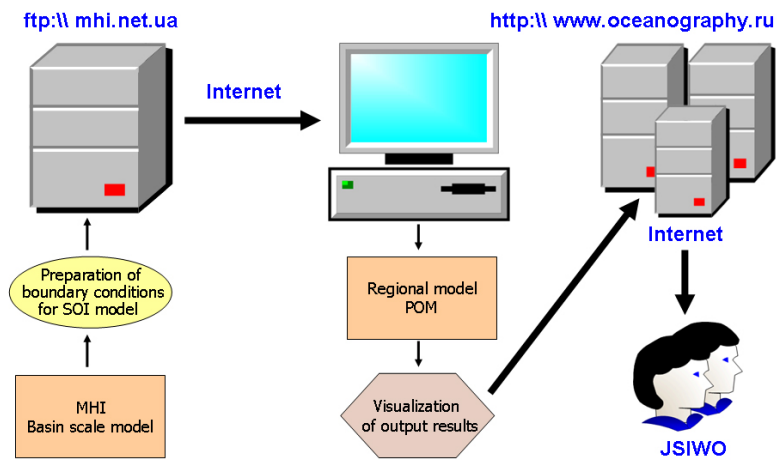


Fig. 3. Scheme of SOI automated system.

1879

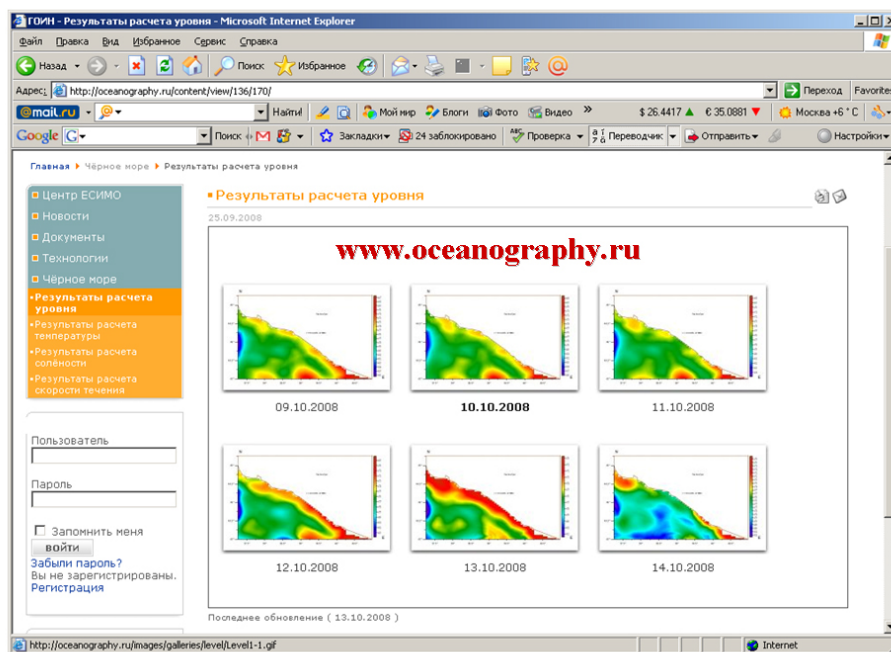
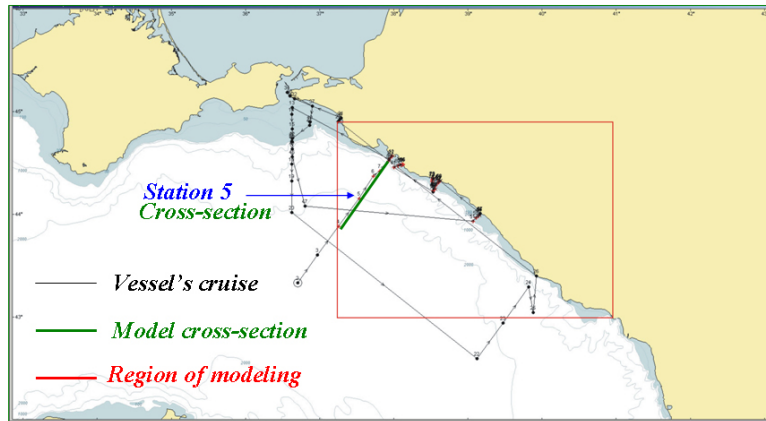


Fig. 4. Example of modeled results shown on the SOI website.

1880





**Fig. 5.** Region of R/V *Professor Shtokman* survey and modeling area.

1881

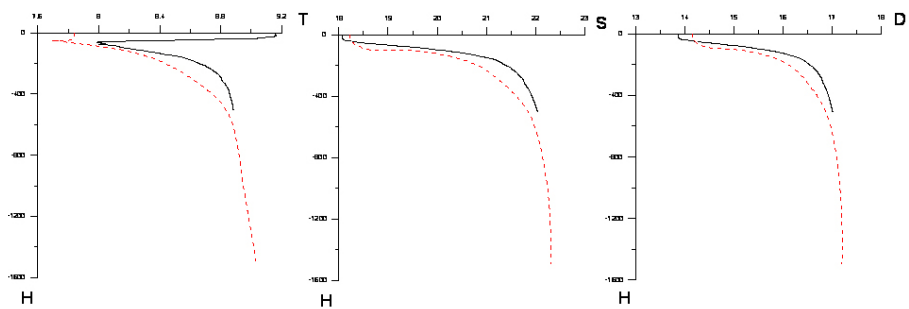


**Fig. 6.** Vertical profiles of temperature ( $T$ ), salinity ( $S$ ) and density ( $D$ ) for Station No. 5 from CTD data (black) and modeling (red).

1882

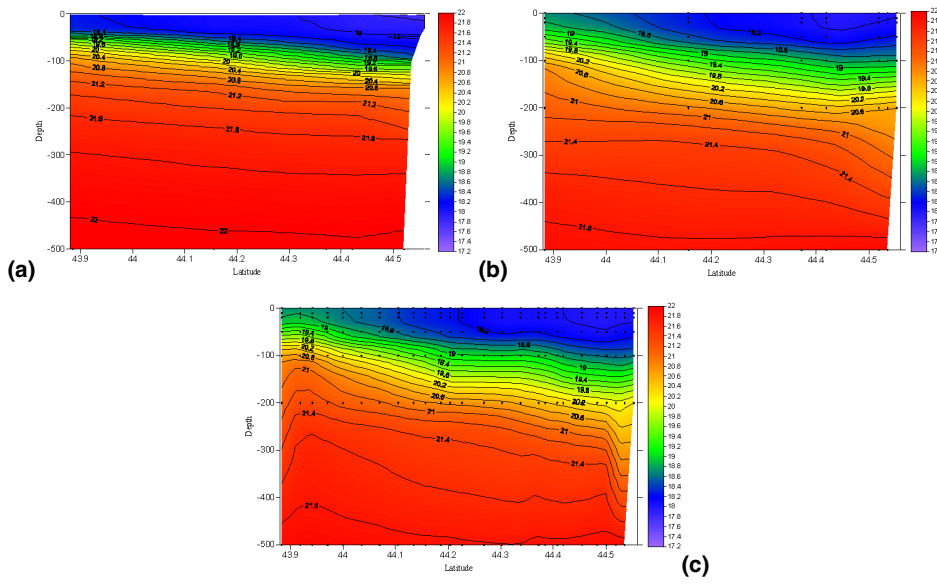


**Fig. 7.** Distribution of salinity on a cross-section (see the Fig. 5), obtained from CTD data (a) and model data (b, c).

1883

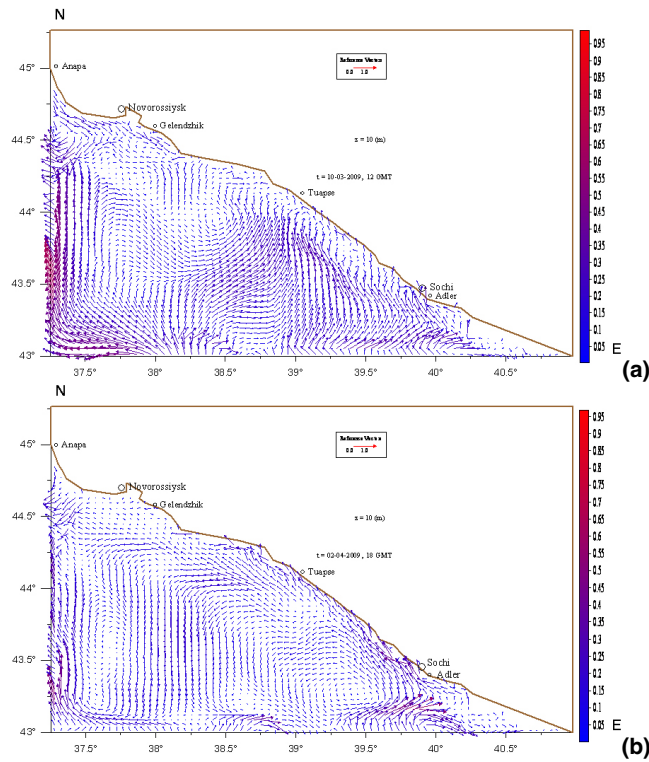


**Fig. 8.** Model fields of sea currents at a depth of 10 m 10/03/2009 (a) and 02/04/2009 (b).

1884

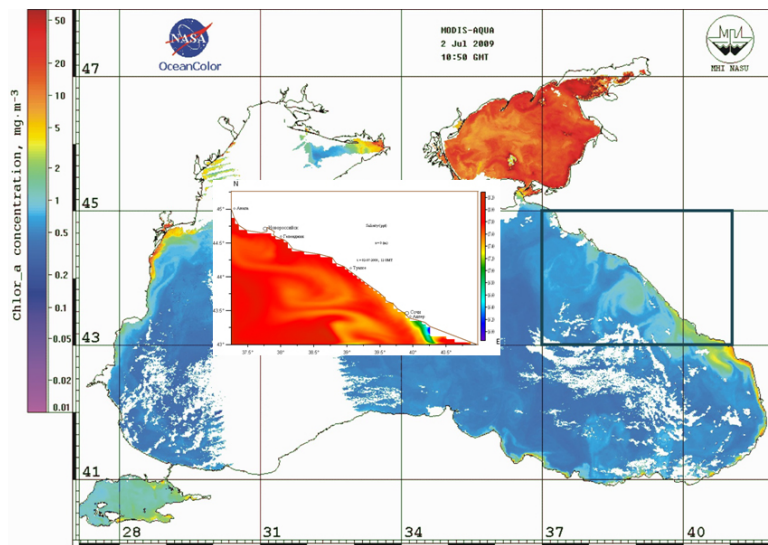


**Fig. 9.** Satellite image (Chlorophyll concentration) and modeled sea surface salinity at 2 July, 2009.

1885

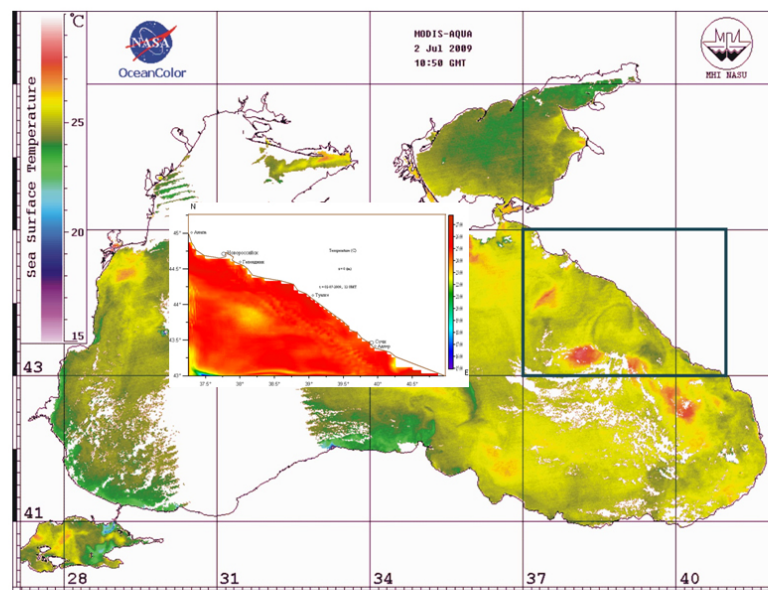


**Fig. 10.** Satellite image (SST) and modeled sea surface temperature at 2 July, 2009.

1886



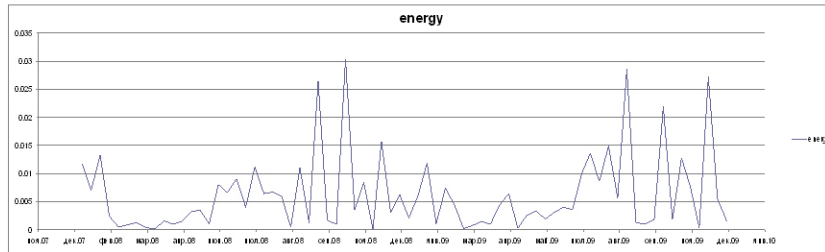


Fig. 13. Average kinetic energy of currents for depth 0 m.

1889

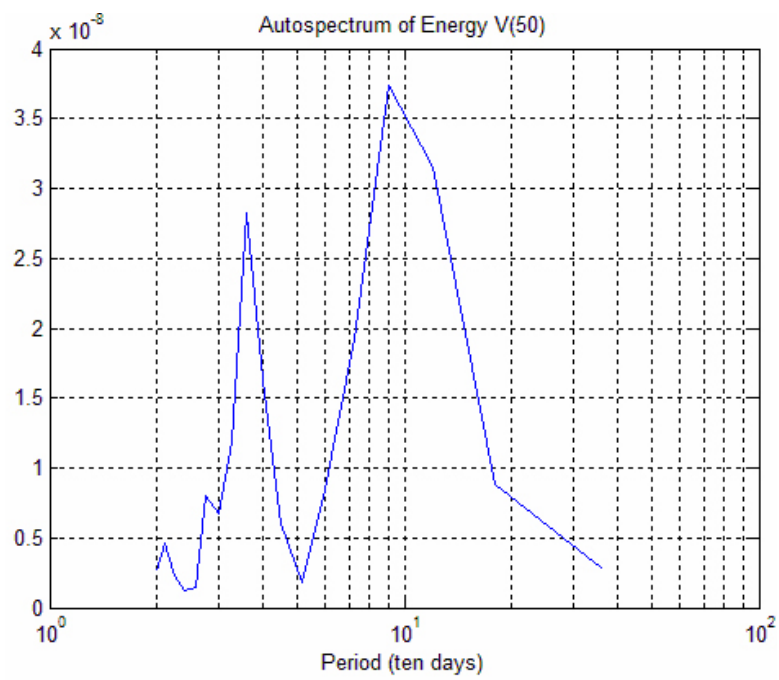


Fig. 14. Autospectrum of kinetic energy of currents for depth 50 m.

1890